Precision Agriculture (2024) 25:1086–1105
https://doi.org/10.1007/s11119-023-10106-9

Estimating canopy chlorophyll in slash pine using multitemporal vegetation indices from uncrewed aerial vehicles (UAVs)

Qifu Luan[1] · Cong Xu[2] · Xueyu Tao[1] · Lihua Chen[3] · Jingmin Jiang[1] · Yanjie Li[1]

Accepted: 2 December 2023 / Published online: 8 January 2024

Abstract
Canopy Chlorophyll Content (CCC) is an important physiological indicator that reflects the growth stage of trees. Accurate estimation of CCC facilitates dynamic monitoring and efficient forest management. In this study, we used high-resolution remote sensing images obtained by uncrewed aerial vehicles (UAVs) equipped with multispectral sensors (red, green, blue, near-infrared, and red-edge) to estimate CCC of lodgepole pine (*Pinus elliottii*). Our aim was to determine the optimal machine learning model between support vector regression (SVR) and random forest regression (RFR) for predicting CCC and to evaluate the effectiveness of multispectral bands along with 21 vegetation indices (VIs) in the estimation process. Individual tree boundaries were derived from the canopy height model (CHM) based on three-dimensional (3D) point clouds generated using structure from motion. These images, combined with continuous field measurements from January to December, provided comprehensive data for our analysis. The results showed that the SVR method outperformed the RFR method in estimating leaf chlorophyll content (LCC), with fitting R^2 values up to 0.692 and RMSE values up to 0.168 $mg \cdot g^{-1}$. Overall, the study highlights the potential of UAV-based remote sensing for multitemporal forest monitoring, offering advances in precision forestry and tree breeding.

Keywords Uncrewed aerial vehicles (UAVs) · Multispectral and multitemporal · Canopy chlorophyll content · Vegetation indices · *Pinus elliottii*

✉ Yanjie Li
aj7105@gmail.com

[1] Research Institute of Subtropical Forestry, Chinese Academy of Forestry (National Forestry and Grassland Engineering Technology Research Center of Exotic Pine Cultivation), No. 73, Daqiao Road, Fuyang, Hangzhou 311400, Zhejiang, China

[2] New Zealand School of Forestry, University of Canterbury, Private Bag 4800, Christchurch 8140, New Zealand

[3] Hangzhou Academy of Forestry Sciences, Hangzhou 310022, Zhejiang, China

Introduction

Chlorophyll content in plant leaves is key factor to understand forest dynamics. As the primary pigment in photosynthetic leaves, chlorophyll is central to the conversion of solar energy into chemical energy. Over the years, research has shown that variations in chlorophyll content can reflect the photosynthetic activity and provide insights into forest health indicators, such as productivity, environmental stress responses, and disease susceptibility (Gitelson et al., 2003, 2006; Ustin et al., 2008).

Given the vast expanse of forests, direct biochemical content estimation at the leaf level is challenging. Consequently, researchers have shifted their focus to canopy-level assessments, with Canopy Chlorophyll Content (CCC) emerging as a crucial metric. CCC, calculated as the product of leaf chlorophyll content (LCC) and leaf area index (LAI), offers insights into the physiological attributes of entire plant communities, making its real-time monitoring essential for applications like yield estimation, pest control, and overall forest growth tracking (Gitelson et al., 2014; Li et al., 2015). Moreover, the interactions of chlorophyll-related pigments and leaf cell structures with light, especially in the 400–1000 nm range, underscore the importance of accurate chlorophyll estimation (Gitelson & Merzlyak, 1997).

The spectrum of a vegetation canopy is influenced by a multitude of factors, including canopy structure, background conditions, solar intensity, and observational angles (Houborg et al., 2009; Zarco-Tejada et al., 2005; Zhang et al., 2008). This multi-faceted influence necessitates a comprehensive approach to chlorophyll estimation at the canopy level, emphasizing the importance of considering leaf health and physiological state, canopy structures, and observational parameters. While traditional methods for measuring canopy chlorophyll content (CCC) are precise, they are labor-intensive, time-consuming, and often invasive (Ciganda et al., 2009; Lichtenthaler & Wellburn, 1983; Zhao et al., 2003). In contrast, remote sensing techniques have proven to be efficient, non-invasive alternatives (Santos et al., 2019).

The realm of optical remote sensing, in particular, has shown promise in estimating vegetation chlorophyll (Clevers, 2012). Recent advancements in research have leveraged spectral data to predict various vegetation traits, emphasizing the importance of monitoring forests using remote sensing methodologies (Gitelson et al., 2014; Kokaly et al., 2009). The evolution of UAVs and their ability to capture multispectral signals has further revolutionized this field, allowing for direct inference of vital plant traits like CCC (Croft et al., 2014; Veronika et al., 2021).

Vegetation indices (VIs), which involve the transformation of two or more bands designed to enhance the contribution of vegetation properties, are crucial due to their flexibility, efficiency, and accuracy in estimating CCC (Verrelst et al., 2015; Wu et al., 2008). They tap into specific wavelength ratios, with some indices even focusing on unique bands sensitive to chlorophyll content (Blackburn, 2007). The integration of multiple VIs often yields more comprehensive insights into leaf chlorophyll at the canopy level (Haboudane et al., 2008; Sun et al., 2021). It is important to note that while many vegetation indices (VIs) are primarily designed to estimate chlorophyll content or other vegetation properties, they can also be responsive to changes in leaf area (Vélez et al., 2023). This sensitivity can result in potential ambiguities in interpretation, particularly when there are simultaneous changes in both chlorophyll content and leaf area (Broge & Leblanc, 2001). For example, indices such as the TGI and NDRE, which are commonly used for chlorophyll estimation, have also been shown to be reactive to fluctuations in leaf area. Recognizing

and accounting for this multisensitivity is essential for accurate vegetation analysis (Barzin et al., 2021).

To further refine these estimations, researchers have increasingly turned to nonlinear models, particularly machine learning regression algorithms (Tuia et al., 2011). Recently, the application of machine learning regression algorithms, such as random forest regression (RFR) (Hastie et al., 2009), deep learning (Chen et al., 2023; Gu et al., 2018), and support vector regression (SVR) (Awad et al., 2015), in forestry has become increasingly widespread. These algorithms, by design, adapt to the data at hand, eliminating the need for prior assumptions and allowing for a more intricate understanding of the relationships within forest ecosystems (Verrelst et al., 2012).

In this study, we aim to establish a comprehensive estimation model for the Canopy Chlorophyll Content (CCC) of slash pine using remote sensing. The overarching goal was to not only delve deeper into the chlorophyll dynamics but also to underscore the potential of UAV spectroscopy in forest monitoring and management. With this context, our study was designed with the following primary objectives:

1. To utilize UAV-based multitemporal and multispectral images to measure the chlorophyll values of slash pine (*Pinus elliottii*) across 11 months.
2. To establish a multispectral remote sensing estimation model of the LCC status of slash pine using VIs.
3. To evaluate the performance of different models and spectral combinations for predicting CCC, aiming to identify the most accurate and efficient approach.

Materials and methods

Study site description

The experiment was conducted in a slash pine plantation located in the Matou national forest farm in Jingxian County, Xuancheng City, Anhui Province, China (30° 45′ N, 118° 29′ E) (Fig. 1). The annual average temperature is 15.7 °C, with January (the coldest month) and July (the hottest month) having daily average temperatures of 2.9 °C and 28.1 °C, respectively. The average annual rainfall is approximately 1525 mm, and the relative humidity is 84%. The soil in the area is predominantly yellow brown soil, with a representative PH value of 5.5–6.0 and soil thickness ranging from 70 to 150 cm. The slash pine plantation covers an area of 6 ha, and is divided into two sites, where 20 open-pollinated families were planted at 2 m × 3 m spacing in 2013.

Ground data acquisition and analysis

Determination of LCC

In order to calculate CCC, the amount of LCC and LAI need to be measured. Field data were collected monthly at the study site from January to December 2021 (excluding February). Throughout the study period, we randomly selected a total of 383 slash pine trees and collected needles from four directions (east, south, west, and north) using a high branch shear tool. The selection intensity varied across months. For instance, December saw intensified sampling due to logistical advantages and supplementary experiments conducted

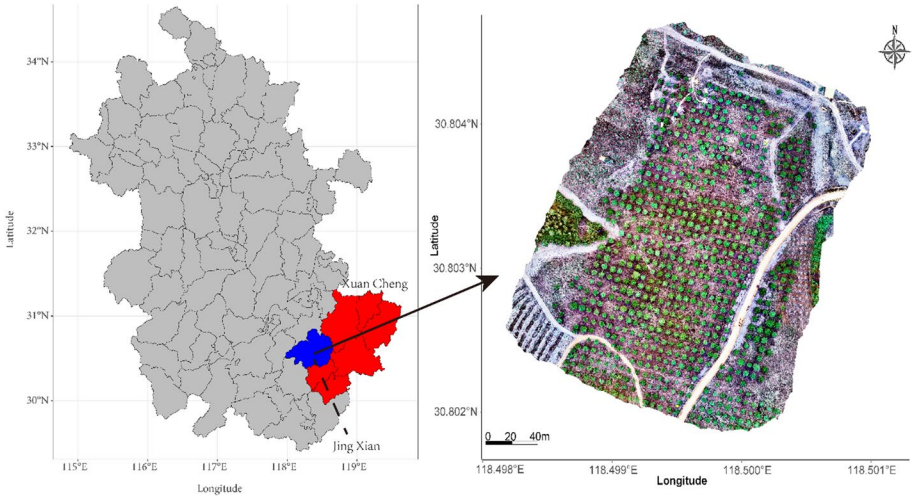

Fig. 1 The Geographic location of the study area and orthomosaic in Xuancheng City, Anhui Province China

during that month. The needles were placed into labeled storage bags and transported to the laboratory in a low-temperature foam box with ice bags. The chlorophyll extraction experiment was performed within 12 h of sample collection to prevent excessive chlorophyll degradation. Needles were cut into pieces, and 0.05 g samples were placed into test tubes with 5 ml of a 1:1 acetone-ethanol solution. The extractions were performed in the dark at room temperature for 24 h. The absorbance of the extracts at wavelengths of 663 nm and 645 nm was read, and the chlorophyll concentration was calculated.

LAI measurements

After capturing the multispectral images on the midday of November 24th, we proceeded to assess the leaf area index (LAI) in the afternoon. From the plantation, we randomly selected 110 slash pines for this purpose.

The LAI was determined using the TOP-1300 Plant Canopy Analyzer from Zhejiang Topu Yunnong Technology Co., Ltd. This instrument uses a fisheye lens with a 150° field of view coupled with a digital camera. Each selected tree was measured three times to ensure accuracy, and an average of the three measurements was recorded for each tree.

For data analysis, the images captured by the analyzer were individually processed using the Hemiview canopy analysis system. The Clumping index (Ω_E) describes the spatial distribution characteristics of the canopy. To account for deviations between the real spatial distribution and the non-random distribution of the canopy, we used a corrected LAI calculation (Chen & Black, 1992; Ma et al., 2018). In such cases, the corrected LAI was computed using Eq. (1) from Chen et al. (1997):

$$\mathrm{LAI} = (1 - a)_* L_{e*} g_E / W_E \tag{1}$$

where:

LAI is the corrected LAI, L_e is the effective LAI from the TOP-1300 optical sensors, Ω_E is the foliage clumping index, a correction factor associated with the vegetation type, γ_E represents the needle-to-shoot ratio, α stands for the woody-to-total area ratio.

For the last three parameters, we adopted published experiential values specific to coniferous forests (Chen & Cihlar, 1996).

UAV multispectral reflectance acquisition

UAV multispectral imaging system

The study employed the DJI Phantom 4 Multispectral (P4M) UAV developed by Dà-Jiāng Innovations Science and Technology Co., Ltd., China, to capture canopy images of slash pine. The camera of the P4M is equipped with six 1/2.9 inch CMOS sensors, consisting of one RGB sensor and five multispectral bands (Table 1), each capable of capturing images at a resolution of 2 megapixels. The camera was oriented perpendicular to the platform, and automatic exposure was used during image acquisition. The P4M was equipped with real-time kinematic (RTK) positioning and navigation, and the ground D-RTK 2 Mobile GNSS Station was utilized to obtain high-precision waypoint positions of the UAV during flight.

Multitemporal multispectral remote sensing images were acquired on 12 January, 24 March, 21 April, 31 May, 23 June, 18 July, 19 August, 17 September, 25 October, 24 November, and 29 December, under clear sky conditions. The flights were conducted between 10:00 and 14:00 local standard time.

The automatic image acquisition was carried out using the DJI Ground Station Pro application (developed by Dà-Jiāng Innovations Science and Technology Co., Ltd., China) in conjunction with a self-provided remote control. The UAV was flown at a height of 35 m above ground level (AGL), with the double grids established to cover the entire plantation area with 80% overlap and 70% side overlap. A standard reflectance panel with a reflectance of 50% was utilized for image radiometric correction during each flight. Consistent UAV parameters and route settings were maintained across all flights.

Individual crown detection

The raw imaging data, including both RGB and multispectral bands, were processed using DJI Terra 3.4.4 software (Dà-Jiāng Innovations Science and Technology Co., Ltd., Shenzhen, China) to generate three-dimensional (3D) point clouds, digital surface models (DSMs) and digital terrain model (DTM) using Structure from Motion and

Table 1 Overview of a P4M spectral band setting

Band name	Center wavelength (nm)	Bandwidth (nm)
Red	650	16
Green	560	16
Blue	450	16
Red-edge	730	16
Near infrared (NIR)	840	26

Multiview Stereo (SfM-MVS) procedures (Navarro et al., 2020). Figure 2 depicts the 3D point clouds of the study site (captured in July).

To create separate canopy height models (CHMs), the DSM was subtracted from the DTM using the max height metric, as described by Navarro et al. (2020). For the purpose of excluding potential non-tree objects, such as shrubs and vehicles, heights less than 2 m were excluded. Depending on the forest's natural conditions, various methods can be used to detect and delineate individual tree crowns (Ke & Quackenbush, 2011; Larsen et al., 2011). In this study, the *lidR* package (Roussel et al., 2020) from R software (Team, 2023) was utilized to compute 3D point clouds and detect individual tree crowns based on their height. Moreover, all detected trees were manually screened and assigned unique identification numbers.

VIs related to physiological index

Vegetation Indices (VIs) effectively minimize the impact of background noise on the spectral characteristics of vegetation, thereby enhancing the precision in deriving vegetation properties from remote sensing data. These indices are derived from linear or nonlinear combinations of reflectance data across different spectral bands. They act as indicators of vegetation health or nutritional status (Modica et al., 2020; Xue & Su, 2017a). In this study, we selected a set of eight VIs, focusing on a range of reflectance patterns linked to chlorophyll and other plant attributes. These VIs are well-established in the literature, highlighting their utility for chlorophyll estimation. Utilizing a variety of VIs, even with potential correlations, enhances the methodological robustness and adaptability, making our model data-rich and versatile for different application scenarios (Table 2).

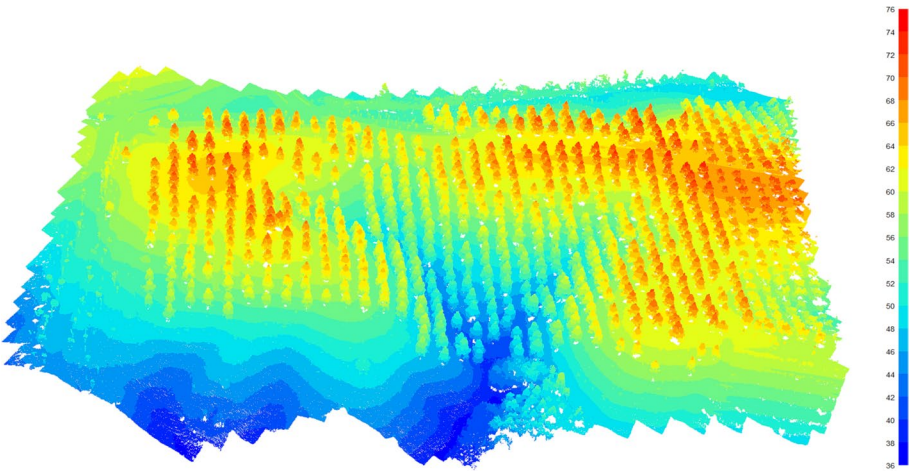

Fig. 2 3D point clouds of a slash pine orchard generated through DJI Terra 2.0 software from the 7490 images acquired by the DJI P4M-UAV platform. Color from blue to red represent the altitude (m) (Color figure online)

Table 2 Details of multispectral VIs related to leaf chlorophyll content (LCC) used in this study

Index	Name	Formula	References
CIRE	Chlorophyll index red-edge	$R_n/R_{re}-1$	Gitelson et al. (2003)
CVI	Chlorophyll vegetation index	$R_n*R_r/{R_g}^2$	Vincini et al. (2008)
EVI	Enhanced vegetation index	$2.5(R_n-R_r)/(R_n+6R_r-7.5R_b+1)$	Huete et al. (2002)
GLI	Green leaf index	$(2R_g-R_r-R_b)/(2R_g+R_r+R_b)$	Louhaichi et al. (2001)
GNDVI	Green normalized difference vegetation index	$(R_n-R_g)/(R_n+R_g)$	Gitelson et al. (1996)
NDVI	Normalized difference vegetation index	$(R_n-R_r)/(R_n+R_r)$	Rouse et al. (1974)
RVI	Ratio vegetation index	R_n/R_r	Pearson and Miller (1972)
TGI	Triangular greenness index	$-0.5[190(R_r-R_g)-120(R_r-R_b)]$	Hunt Jr et al. (2011)

Rr, Rg, Rb, Rre, and Rn are the reflectance for the red, green, blue, red-edge and near-infrared bands, respectively

Statistical methods

Model calibration and prediction

Machine learning methods have become increasingly popular in recent years due to their ability to characterize trends between variables, even when samples are not linearly separable, making them more effective than traditional linear regression methods. In this study, two supervised regression models, support vector regression (SVR) and random forest regression (RFR), were used to predict LAI and LCC, which are fundamental variables for estimating Canopy Chlorophyll Content (CCC). These regression models were fitted and tuned using the *e1071* (Meyer et al., 2015) and *randomForest* (Liaw & Wiener, 2002) packages in R Studio software (Integrated Development for R. R Studio, Inc., Boston, MA). Two regression tests were performed to quantify the estimation capability for the final estimation of LCC, with the measured LCC values used as dependent variables and the spectral and VI data used as explanatory variables.

For both models, we started with hyper-parameter optimization to ensure that optimal parameters were set to avoid overfitting and to ensure accurate prediction performance of the trained model. SVR is a type of supervised machine learning algorithm. It works by mapping input data into a high-dimensional space and then finding a hyperplane that best fits the data. The optimal hyperplane is the one that has the maximum distance from any point in the training data. The term "universality in high-dimensional space" refers to SVR's ability to handle data sets that aren't linearly separable by transforming them into a higher dimension where they become separable. The transformation is often performed using kernel functions (Cutler et al., 2004). RFR, on the other hand, is an ensemble learning method that works by constructing a "forest" of decision trees during training. It then outputs the mode of the classes (classification) or the mean prediction (regression) of the individual trees for unseen data. A notable feature of RFR is its ability to rank the importance of variables, making it valuable for feature selection. In addition, RFR is known to be robust to overfitting and relatively insensitive to collinearity between variables (Breiman et al., 2015).The Classification and Regression Tree (CART) method used in RFR typically uses the Gini index to measure data impurity

or uncertainty, providing insight into the inherent feature selection of the RFR model (Menze et al., 2009).

Accuracy assessment

In this study, we utilized the coefficient of determination (R^2, Eq. (2)) and the root mean square error (RMSE, Eq. (3)) as accuracy verification indicators to evaluate the quality of the model prediction. Generally, R^2 values range from 0 to 1, and higher values indicate better performance of the prediction model. On the other hand, RMSE reflects the level of deviation between the predicted and measured values, and smaller RMSE values indicate higher accuracy of the prediction model.

$$R^2 = 1 - \frac{\sum_{i=1}^{n} (yi - \hat{y}i)^2}{\sum_{i=1}^{n} \left(yi - \bar{y}i\right)^2} \tag{2}$$

$$RMSE = \sqrt{\frac{\sum_{i=1}^{n} (yi - \hat{y}i)^2}{n}} \tag{3}$$

where n is the number of samples, yi is the observed value, $\hat{y}i$ is the predicted value and $\bar{y}i$ is the mean of the observed values.

Results

Canopy extraction and ground truth data

The 3D point cloud of the experimental forest was obtained and the canopy spectral information for each tree was extracted based on their respective canopy area information. As shown in Fig. 3, each polygon area represents the canopy area of a tree, with a unique tree ID assigned. Based on this canopy area information, we performed single-tree processing of the multi-spectral data for each multispectral channel, and extracted the canopy spectral information for each tree, using data from July as an example. Table 3 provides the ground-measured LCC values for the 383 trees across different months, detailing the minimum, maximum, and mean concentrations of chlorophyll. The variability observed in these measurements is instrumental for the development of a predictive model for chlorophyll content. The diverse range of LCC values captured throughout the seasons enriches the dataset, allowing the model to accommodate and predict chlorophyll fluctuations with greater accuracy and reliability.

LAI models using VIs of slash pine

Figure 4 illustrates the calibration and validation performance of the SVR and RF models in predicting LAI. The SVR model exhibits robust calibration with an R^2 of 0.90 and an RMSE of 0.22, denoting a substantial fit to the training data with moderate prediction error. In the validation phase, the SVR model maintains high predictive precision, evidenced by an R^2 of 0.94 and a reduced RMSE of 0.07, indicating enhanced model performance on unseen data.

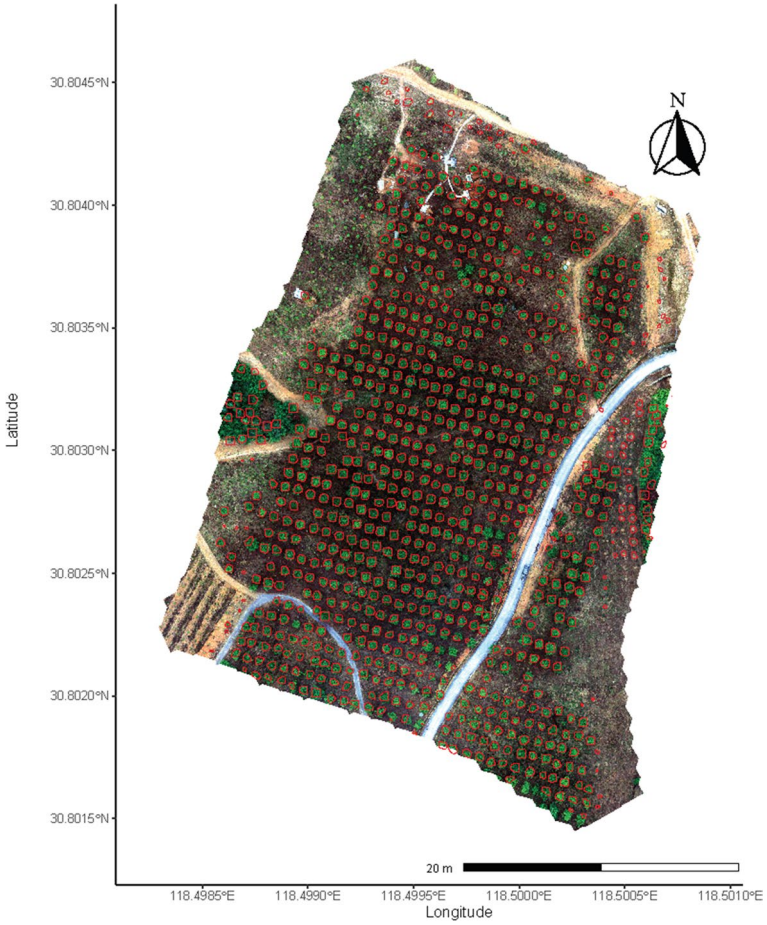

Fig. 3 The corresponding areas extracted from the single-band images of the multispectral data for each tree (data from July)

Table 3 Summary of LCC measured values on the ground of all 383 trees in the study area

Month	Number	LCC (mg/g)		
		Min	Max	Mean
March	28	0.53	1.51	1.02
April	45	0.49	1.63	1.14
May	41	0.80	2.38	1.36
June	37	1.02	2.03	1.46
July	18	0.49	1.24	0.78
August	21	0.58	1.01	0.74
September	28	0.67	1.07	0.85
October	30	0.61	1.4	0.84
November	30	0.67	1.22	0.53
December	105	0.40	1.41	0.83

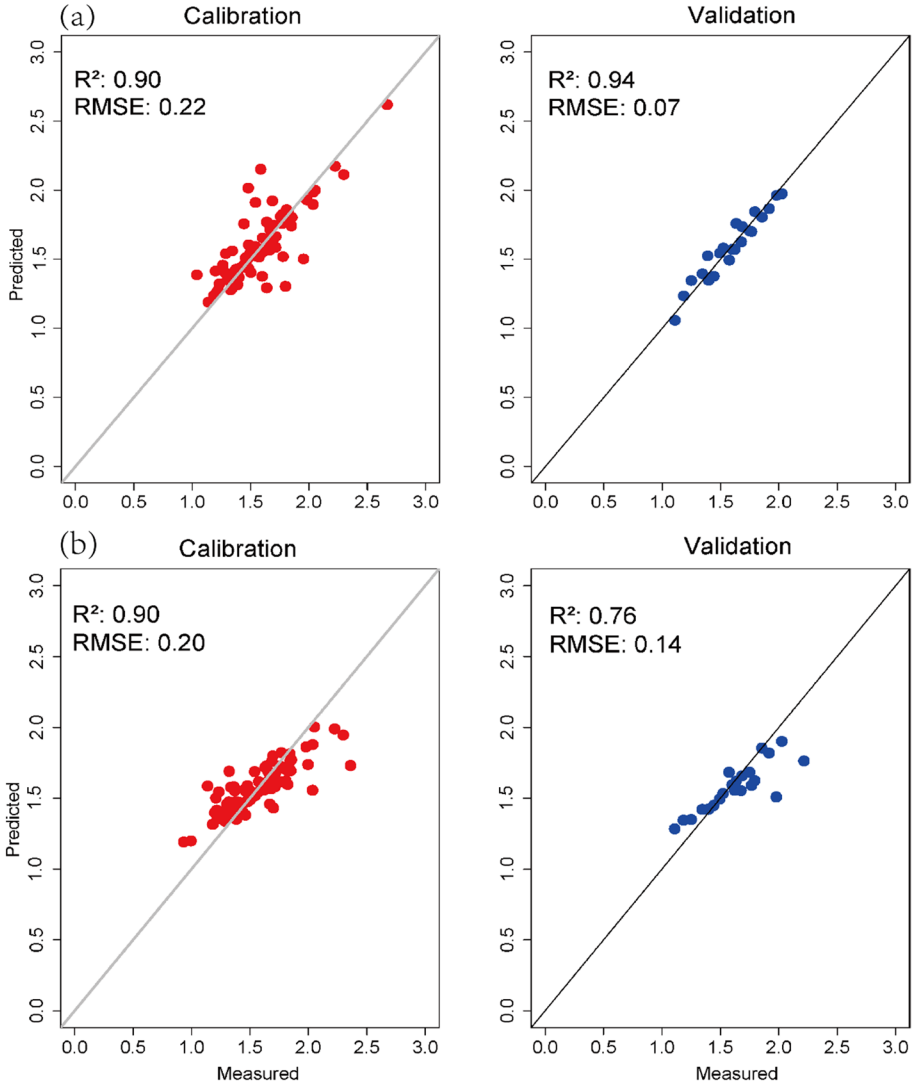

Fig. 4 Calibration (Red) and validation (Blue) scatter plots indicating predictive accuracy of SVR (**a**) and RF (**b**) models for LAI with R^2 and RMSE metrics (Color figure online)

In contrast, the RF model shows a comparable calibration R^2 of 0.90, but with a marginally lower RMSE of 0.20. Nonetheless, its validation performance indicates a decrease in predictive accuracy (R^2 of 0.76) and an increased RMSE of 0.14, suggesting a diminished generalizability to new data compared to the SVR model. Although both models demonstrate strong calibration capabilities, the SVR model exhibits superior validation performance, as reflected by the higher R^2 and lower RMSE metrics.

LCC Models using multispectral and VIs of slash pine

After outlier detection and removal, where data points greater than 1.5 times the interquartile range (IQR) above the third quartile or below the first quartile were excluded, three data points were discarded. An 80% random subset of the sample trees was allocated for the training set, with the remaining 20% forming the validation set. Both the SVR and RFR models demonstrated consistent performance in all-index modeling. Figure 5 presents scatter plots comparing measured versus predicted LCC values across various months, with the calibration set results on the left and the validation set results on the right. The analysis employed two machine learning approaches: SVR shown on the top, and RFR displayed on the bottom. For the SVR, the calibration and validation sets yielded R^2 values of 0.68 and 0.70, with RMSEs of 0.16 mg/g for both sets. The RF model exhibited R^2 values of 0.90 for calibration and 0.81 for validation, with corresponding RMSEs of 0.08 mg/g and 0.17 mg/g, respectively.

Figure 6 presents residual plots for the SVR and RF calibration and validation models for slash pine. These plots allow for the assessment of the linear relationship between the predicted LCC values and the residuals. The residuals are observed to be randomly distributed around the zero line, indicating no apparent systematic error in the predictions. The spread of residuals is narrower than initially described, lying within approximately ± 0.4 for both models, which suggests an improvement in model precision. The residual patterns

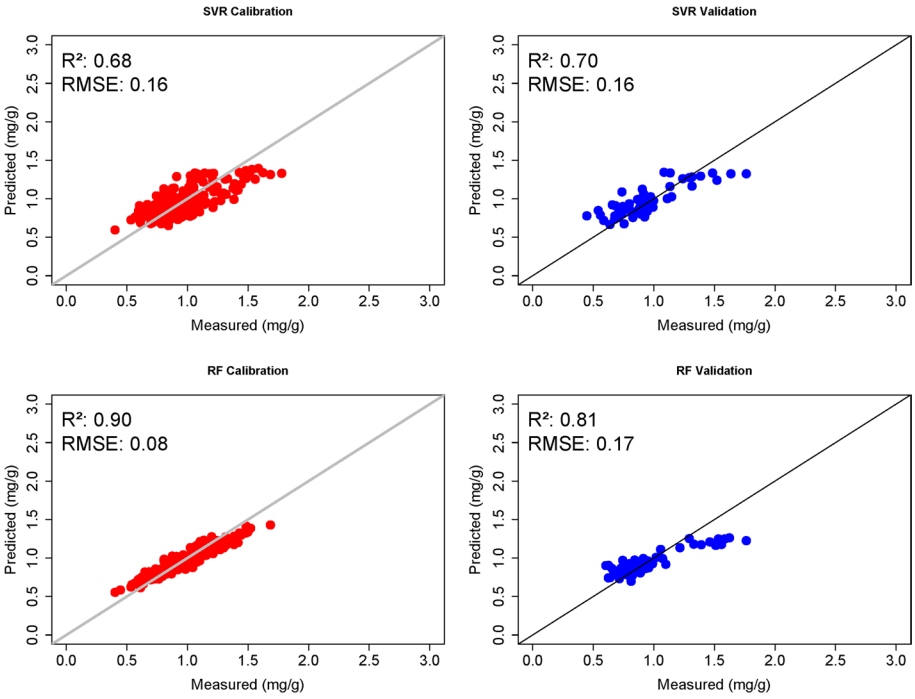

Fig. 5 Comparative scatter plots of measured vs. predicted LCC in slash pine using SVR on the Top and RFR on the Bottom. The left scatter plots represent the calibration set and the right scatter plots represent the validation set. The plots illustrate the relationship between measured (x-axis) and predicted (y-axis) LCC values

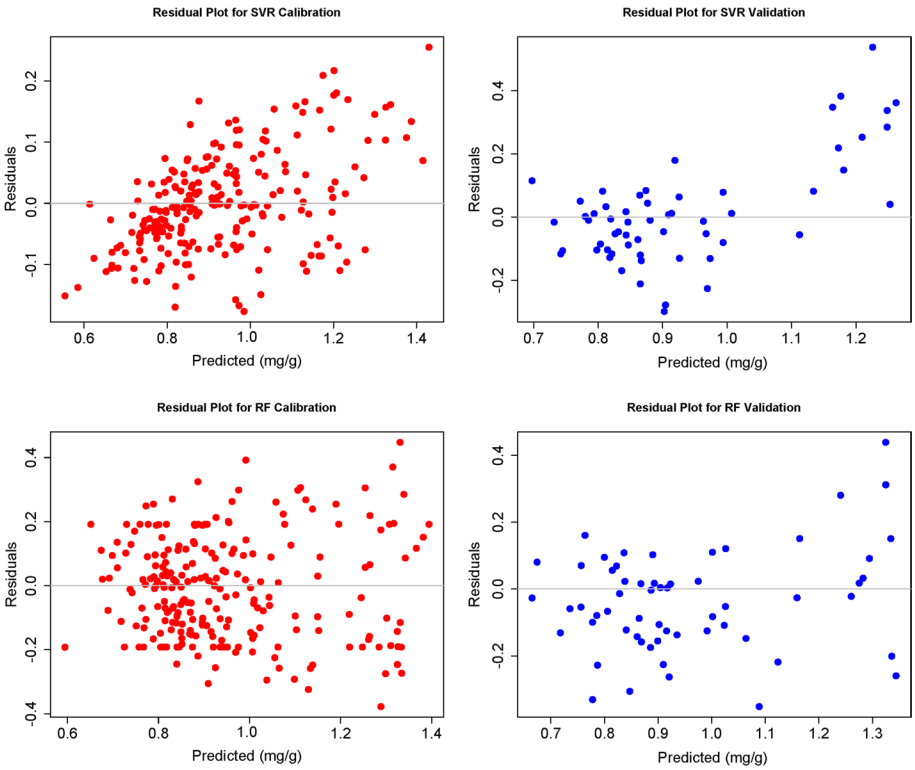

Fig. 6 Residual distribution for SVR and RF models in LCC prediction of slash pine across calibration and validation sets

do not exhibit a clear increasing trend with the predicted LCC values, which contrasts with previous observations. The RF model appears to have a tighter clustering of residuals around zero, especially in the calibration phase, indicating a potentially better model fit compared to the SVR model. Consequently, the RF model should be considered for the next steps in CCC prediction.

Figure 7 illustrates the variable importance for LCC as determined by RFR model. The TGI is shown to have the highest importance value, indicating its significant role in the model's predictions. It is followed by the RVI and the NDVI, both of which also contribute notably to the model. The GNDVI and the CIRE occupy the middle range of importance values. The GLI and the EVI appear to have a lower relative importance in this model. The CVI is observed to have the least importance among the variables presented.

Multitemporal estimation and mapping of slash pine CCC using multispectral imagery

Figure 8 depicts the results of RFR model used to predict the monthly canopy chlorophyll content (CCC) of individual slash pine trees within the plantation. Each point in the plot represents a single tree, with the spatial distribution of points corresponding to the actual positions of the trees within the plantation. From the onset of January, the CCC values are

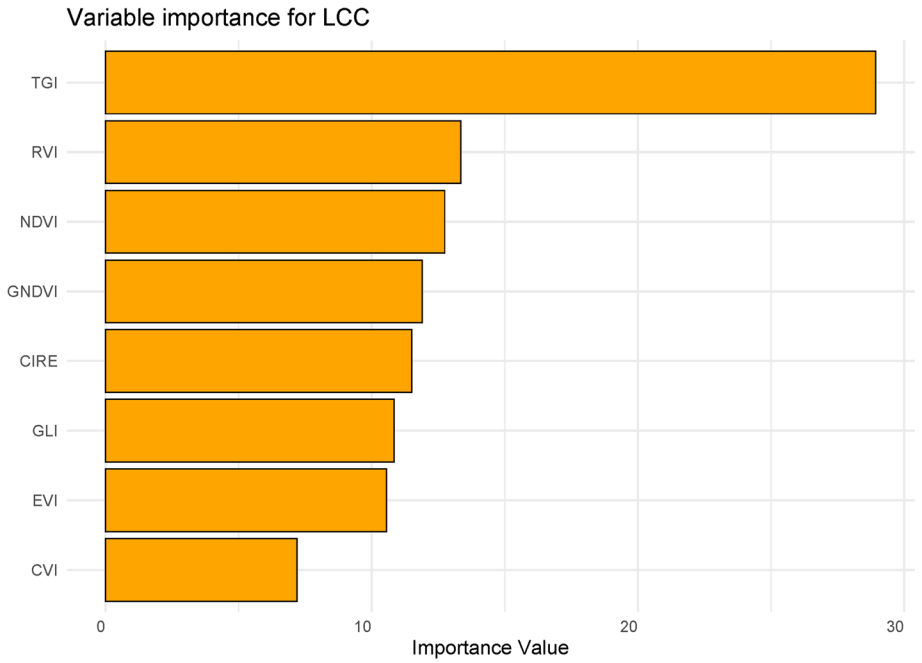

Fig. 7 The ranking of importance for the top 10 predictor variables of leaf chlorophyll content (LCC) based on RFR, which explained the mean increase in node purity (i.e., decrease in node impurity: Gini Index)

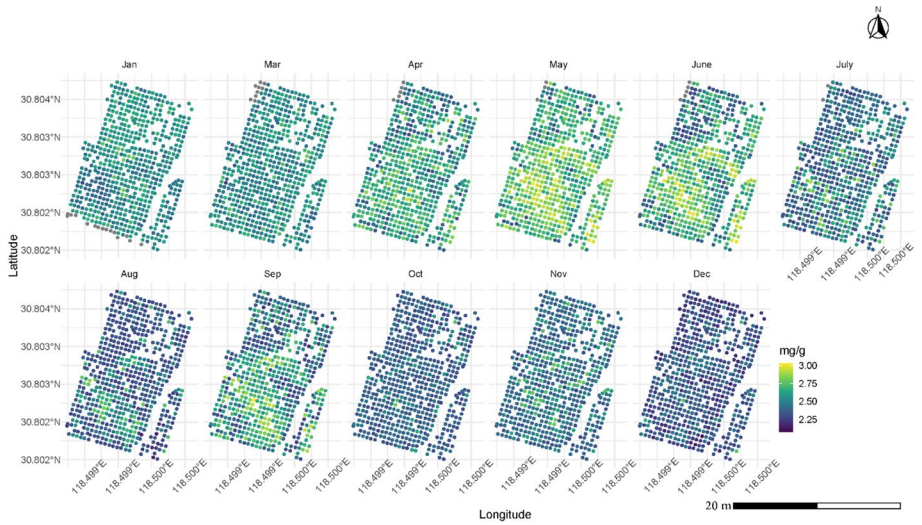

Fig. 8 Multitemporal prediction results of slash pine CCC based on RFR

generally low, aligning with the cooler climatic conditions. As the temperature gradually rises, there is a noticeable increment in the CCC of the slash pine canopy, particularly during May and June, where many trees reach their peak chlorophyll content. This period of maximal CCC is followed by a decline in July and August. However, a subsequent increase is observed in September, suggesting a temporary resurgence in chlorophyll concentration. From October onwards, the CCC begins to decrease again, indicating a seasonal downward transition.

Discussion

While there is limited research that addresses the prediction of chlorophyll content concentration (CCC) for *Pinus elliottii* using remote sensing techniques, our study utilizes multitemporal and multispectral UAV imagery to fill this gap. By considering a wide range of canopy physiological and structural parameters, we use different vegetation indices (VIs) to assess chlorophyll content at the canopy scale.

Variable selections

The application of vegetation indices (VIs) within Random Forest Regressor (RFR) models is crucial for accurate Leaf Chlorophyll Content (LCC) estimation, as demonstrated by multispectral data's role as a non-destructive tool reflecting photosynthetic efficiency (Glenn et al., 2008; Xue & Su, 2017b). These indices provide valuable insights into vegetation responses to environmental and ecological changes, as they are indicative of CO2 uptake and photosynthetic processes (Gupana et al., 2021). In our RFR model, the Triangular Greenness Index (TGI) was identified as the most significant variable, strongly correlated with the spectral bands around 700 nm, essential for LCC prediction. Furthermore, the spectral ranges of 500–550 nm and 600–700 nm, commonly associated with VIs, have been affirmed as critical for accurate LCC prediction (Jiao et al., 2023).

The analysis emphasizes TGI's sensitivity to chlorophyll content within the slash pine canopy, confirming findings by Hunt Jr et al. (2011). RVI and NDVI also emerged as significant, resonating with their established correlation with vegetative vigor (Sims & Gamon, 2002). Conversely, the Chlorophyll Vegetation Index (CVI) showed the least significance, suggesting its limited responsiveness to the spectral characteristics of slash pine and highlighting the need for further investigation into its application (Vincini & Frazzi, 2011; Vincini et al., 2007). Our research thus enhances the selection process of spectral indices for LCC estimation and underscores the importance of developing species-specific remote sensing applications in forestry (Gao et al., 2022; Li et al., 2019). Future studies should persist in appraising the empirical significance of these indices across diverse forest ecosystems.

Model comparison

In our study, the RFR model outperformed other models for retrieving LAI values. The results indicated that RFR effectively handled the limited spectral information and reduced vulnerabilities from background interferences. This emphasizes the strength of the RFR model in optimizing canopy spectral information, leading to more accurate estimations of

LAI. Our findings align with the benefits of machine learning methods in addressing such challenges, as highlighted by (Osco et al., 2019).

Machine learning methods are more resistant to problems caused by highly correlated variables compared to multiple linear regression (MLR) models, which make them suitable for anticipating multitemporal canopy physiological indicators with UAV multispectral imagery (Garcia-Gutierrez et al., 2014). Nevertheless, it should be acknowledged that even though these methods handle multicollinearity more efficiently, they are not completely free of its consequences. The algorithms utilized in this research demonstrate high correlations, which may result in some overlap; however, we sought to encompass a wide array of data. Our findings indicate that both SVR and RFR techniques have potential in forecasting LCC. The RFR model delivered exceptional outcomes both in the calibration and validation process, highlighting its efficacy as an anticipatory instrument for UAV multispectral data obtained over slash pine forests.

These conclusions are further supported by similar studies. For instance, research combining fixed-wing UAV multispectral imagery and machine learning to diagnose winter wheat nitrogen status at the farm scale used similar methodologies, supporting our findings regarding the utility of RFR models in agricultural analysis (Jiang et al., 2022). Additionally, other studies have emphasized the effectiveness of RFR in the estimation of transpiration coefficients and aboveground biomass using UAV multispectral images (Shao et al., 2022), as well as in the prediction of maize crop coefficient from UAV multisensor remote sensing (Shao et al., 2023). A study on unsupervised plot-scale LAI phenotyping via UAV-based imaging also developed a method to train RFR models for estimating LAI from UAV-based multispectral images, which aligns closely with our research objectives and findings (Chen et al., 2022).

Monthly variations of CCC

The multitemporal monitoring revealed distinct trends in canopy-integrated chlorophyll content (LAI × LCC) of slash pine throughout the year. The specific characteristics of *Pinus elliottii* as an evergreen conifer played an important role in these observations. For example, we observed that the CCC of slash pine, which by nature has little monthly variation, had higher values in the summer than in the winter. This trend is consistent with the natural behavior of the species, as documented in previous studies (Curran et al., 1992a; Sumida et al., 2019). Furthermore, the observed insensitivity of sunlight penetration to changes in slash pine leaf area can be attributed to its highly clumped canopy structure (Gholz et al., 1991). Such findings underscore the reliability and accuracy of our approach, which is in good agreement with the existing literature (Iiames et al., 2008).

We found that the CCC showed an upward trend followed by a downward trend, peaking in May. This phenomenon can be explained by the growth rhythm of slash pine trees. Sprouting of slash pine trees begins in late March, and the outbreak and growth of new shoots can be observed in June. The two-year-old cohorts defoliate in September (Hakala et al., 2015). Therefore, we found that one-year-old needles reach their growth peak at the end of May, accounting for the largest proportion in the canopy, while the proportion of current-year needles expands. In July and August, the canopy needles of slash pine consist almost entirely of new needles from the current year. At this time, the age distribution of needles in the canopy is more complicated, which is why the numerical values of CCC are most scattered in summertime. In September, the new needles have accumulated chlorophyll through photosynthesis, causing a slight increase in foliage chlorophyll content

compared to before. It should be noted that CCC is lower in current-year leaves than in one-year-old leaves (Katahata et al., 2007; Wang et al., 2020), which our study confirmed.

The importance of multitemporal observations in capturing dynamic changes in plant physiology at the canopy scale has been well established in previous studies. For instance, Hakala et al. (2015) highlighted the potential of multispectral lidar in capturing seasonal and spatial variations in chlorophyll content of Scots pine. In our study, understanding the reflectance properties of leaves revealed a strong correlation between biochemical concentrations, such as CCC, and radiation reflectance in specific spectral regions (Curran, 1989). Such relationships are influenced by several factors, including electronic transitions in pigments and specific molecular vibrations (Card et al., 1988; Curran et al., 1992b). Thus, changes in vegetation cover or the external environment can lead to variations in reflectance properties. This underscores the need for multitemporal observations to provide a holistic understanding of plant growth patterns and ensure a robust and stable model.

Conclusion

Multitemporal estimation of forest physiological traits using UAV multispectral imagery has emerged as a highly efficient and portable remote sensing tool for forestry. In this paper, we have explored the feasibility of estimating canopy-integrated CCC, LAI, and LCC of slash pine at the canopy scale from January to December using two machine learning modeling methods, SVR and RFR. Our study has utilized several multispectral bands, VIs, integrated multispectral imagery and 3D point cloud data based on the UAV platform. Overall, our findings reveal that RFR outperformed SVR in LCC modeling due to its stability. Several variables, including TGI, RVI, NDVI, GNDVI and CIRE, were highly influential for RFR modeling in LCC estimation. In conclusion, this study demonstrates that UAV-based remote sensing approaches can effectively predict slash pine CCC at the tree level with high throughput and have the potential for multitemporal remote monitoring of CCC for slash pine. In the long term, conducting more in-depth studies on the relevance between forest physiological traits and VIs derived from UAV-based multispectral digital cameras and related approaches could provide valuable insights into future trends in precision forestry and tree breeding.

Author contributions QL and XT conducted the experiment and wrote the manuscript. YL designed the study, supervised experiments, supported the data collection and performed revisions of the manuscript. CX, LC and JJ revised the manuscript, and all authors read and approved the final manuscript.

Funding This work was supported by the Science and Technology Innovation 2030-Agricultural Biological Breeding Major Project (2023ZD040580105), Fundamental Research Funds of Chinese Forestry Academy (CAFYBB2022QA001) and Zhejiang Science and Technology Major Program on Agricultural New Variety Breeding (2021C02070-8).

Data availability The data used for this paper is freely available upon permission of Research Institute of Subtropical Forestry, Chinese Academy of Forestry.

Declarations

Competing interests The authors declare that they do not know of any competing financial interests or personal relationships that could have appeared to influence the work reported in this paper.

References

Awad, M., Khanna, R., Awad, M., & Khanna, R. (2015). Support vector regression. *Efficient Learning Machines: Theories, Concepts, and Applications for Engineers and System Designers*. https://doi.org/10.1007/978-1-4302-5990-9

Barzin, R., Kamangir, H., & Bora, G. C. (2021). Comparison of machine learning methods for leaf nitrogen estimation in corn using multispectral UAV images. *Transactions of the ASABE, 64*, 2089–2101.

Blackburn, G. A. (2007). Hyperspectral remote sensing of plant pigments. *Journal of Experimental Botany, 58*, 855–867.

Breiman, L. I., Friedman, J. H., Olshen, R. A., & Stone, C. J. (2015). Classification and regression trees. *Encyclopedia of Ecology, 57*, 582–588.

Broge, N. H., & Leblanc, E. (2001). Comparing prediction power and stability of broadband and hyperspectral vegetation indices for estimation of green leaf area index and canopy chlorophyll density. *Remote Sensing of Environment, 76*, 156–172.

Card, D. H., Peterson, D. L., Matson, P. A., & Aber, J. D. (1988). Prediction of leaf chemistry by the use of visible and near infrared reflectance spectroscopy. *Remote Sensing of Environment, 26*, 123–147.

Chen, B., Wang, L., Fan, X., Bo, W., Yang, X., & Tjahjadi, T. (2023). Semi-FCMNet: Semi-supervised learning for forest cover mapping from satellite imagery via ensemble self-training and perturbation. *Remote Sensing, 15*, 4012.

Chen, J. M., & Black, T. A. (1992). Foliage area and architecture of plant canopies from sunfleck size distributions. *Agricultural and Forest Meteorology, 60*, 249–266.

Chen, J. M., & Cihlar, J. (1996). Retrieving leaf area index of boreal conifer forests using landsat TM images. *Remote Sensing of Environment, 55*, 153–162.

Chen, J. M., Rich, P. M., Gower, S. T., Norman, J. M., & Plummer, S. (1997). Leaf area index of boreal forests: Theory, techniques, and measurements. *Journal of Geophysical Research Atmospheres, 102*, 29429–29443.

Chen, Q., Zheng, B., Chenu, K., Hu, P., & Chapman, S. C. (2022). Unsupervised plot-scale LAI phenotyping via UAV-based imaging, modelling, and machine learning. *Plant Phenomics*. https://doi.org/10.34133/2022/9768253

Ciganda, V., Gitelson, A., & Schepers, J. (2009). Non-destructive determination of maize leaf and canopy chlorophyll content. *Journal of Plant Physiology, 166*, 157–167.

Clevers, J. (2012). Using hyperspectral remote sensing data for retrieving canopy chlorophyll and nitrogen content. *IEEE Journal of Selected Topics in Applied Earth Observations and Remote Sensing, 5*, 574–583.

Croft, H., Chen, J., & Zhang, Y. (2014). The applicability of empirical vegetation indices for determining leaf chlorophyll content over different leaf and canopy structures. *Ecological Complexity, 17*, 119–130.

Curran, P. J. (1989). Remote sensing of foliar chemistry. *Remote Sensing of Environment, 30*, 271–278.

Curran, P. J., Dungan, J. L., & Gholz, H. L. (1992a). Seasonal LAI in slash pine estimated with Landsat TM. *Remote Sensing of Environment, 39*, 3–13.

Curran, P. J., Dungan, J. L., Macler, B. A., Plummer, S. E., & Peterson, D. L. (1992b). Reflectance spectroscopy of fresh whole leaves for the estimation of chemical concentration. *Remote Sensing of Environment, 39*, 153–166.

Cutler, A., Cutler, D. R., & Stevens, J. R. (2004). Random forests. *Machine Learning, 45*, 157–176.

Gao, D., Qiao, L., An, L., Zhao, R., Sun, H., Li, M., Tang, W., & Wang, N. (2022). Estimation of spectral responses and chlorophyll based on growth stage effects explored by machine learning methods. *The Crop Journal, 10*, 1292–1302.

Garcia-Gutierrez, J., Martínez-Álvarez, F., Troncoso, A., & Riquelme, J.C. (2014). A comparative study of machine learning regression methods on LiDAR data: A case study. In, *International Joint Conference SOCO'13-CISIS'13-ICEUTE'13* (pp. 249–258): Springer

Gholz, H., Vogel, S., Cropper, W., Jr., McKelvey, K., Ewel, K., Teskey, R., & Curran, P. (1991). Dynamics of canopy structure and light interception in Pinus elliottii stands, North Florida. *Ecological Monographs, 61*, 33–51.

Gitelson, A. A., Gritz, Y., & Merzlyak, M. N. (2003). Relationships between leaf chlorophyll content and spectral reflectance and algorithms for non-destructive chlorophyll assessment in higher plant leaves. *Journal of Plant Physiology, 160*, 271.

Gitelson, A. A., Kaufman, Y. J., & Merzlyak, M. N. (1996). Use of a green channel in remote sensing of global vegetation from EOS-MODIS. *Remote Sensing of Environment, 58*, 289–298.

Gitelson, A. A., & Merzlyak, M. N. (1997). Remote estimation of chlorophyll content in higher plant leaves. *International Journal of Remote Sensing, 18*, 2691–2697.

Gitelson, A. A., Peng, Y., Arkebauer, T. J., & Schepers, J. (2014). Relationships between gross primary production, green LAI, and canopy chlorophyll content in maize: Implications for remote sensing of primary production. *Remote Sensing of Environment, 144*, 65–72.

Gitelson, A. A., Viña, A., Verma, S. B., Rundquist, D. C., Arkebauer, T. J., Keydan, G., Leavitt, B., Ciganda, V., Burba, G. G., & Suyker, A. E. (2006). Relationship between gross primary production and chlorophyll content in crops: Implications for the synoptic monitoring of vegetation productivity. *Journal of Geophysical Research: Atmospheres*. https://doi.org/10.1029/2005JD006017

Glenn, E. P., Huete, A. R., Nagler, P. L., & Nelson, S. G. (2008). Relationship between remotely-sensed vegetation indices, canopy attributes and plant physiological processes: What vegetation indices can and cannot tell us about the landscape. *Sensors, 8*, 2136–2160.

Gu, J., Wang, Z., Kuen, J., Ma, L., Shahroudy, A., Shuai, B., Liu, T., Wang, X., Wang, G., & Cai, J. (2018). Recent advances in convolutional neural networks. *Pattern Recognition, 77*, 354–377.

Gupana, R. S., Odermatt, D., Cesana, I., Giardino, C., Nedbal, L., & Damm, A. (2021). Remote sensing of sun-induced chlorophyll-a fluorescence in inland and coastal waters: Current state and future prospects. *Remote Sensing of Environment, 262*, 112482.

Haboudane, D., Tremblay, N., Miller, J. R., & Vigneault, P. (2008). Remote estimation of crop chlorophyll content using spectral indices derived from hyperspectral data. *IEEE Transactions on Geoscience & Remote Sensing, 46*, 423–437.

Hakala, T., Nevalainen, O., Kaasalainen, S., & Mäkipää, R. (2015). Multispectral lidar time series of pine canopy chlorophyll content. *Biogeosciences, 12*, 1629–1634.

Hastie, T., Tibshirani, R., Friedman, J., Hastie, T., Tibshirani, R., & Friedman, J. (2009). *Random forests. The elements of statistical learning: Data mining, inference, and prediction* (pp. 587–604). Springer.

Houborg, R., Anderson, M., & Daughtry, C. (2009). Utility of an image-based canopy reflectance modeling tool for remote estimation of LAI and leaf chlorophyll content at the field scale. *Remote Sensing of Environment, 113*, 259–274.

Huete, A., Didan, K., Miura, T., Rodriguez, E. P., Gao, X., & Ferreira, L. G. (2002). Overview of the radiometric and biophysical performance of the MODIS vegetation indices. *Remote Sensing of Environment, 83*, 195–213.

Hunt, E. R., Jr., Daughtry, C. S. T., Eitel, J. U. H., & Long, D. S. (2011). Remote sensing leaf chlorophyll content using a visible band index. *Agronomy Journal, 103*, 1090–1099.

Iiames, J., Congalton, R. G., Pilant, A. N., & Lewis, T. E. (2008). Leaf area index (LAI) change detection analysis on Loblolly pine (Pinus taeda) following complete understory removal. *Photogrammetric Engineering & Remote Sensing, 74*, 1389–1400.

Jiang, J., Atkinson, P. M., Zhang, J., Lu, R., Zhou, Y., Cao, Q., Tian, Y., Zhu, Y., Cao, W., & Liu, X. (2022). Combining fixed-wing UAV multispectral imagery and machine learning to diagnose winter wheat nitrogen status at the farm scale. *European Journal of Agronomy, 138*, 126537.

Jiao, Q., Zhang, B., Huang, W., Ye, H., Zhang, Z., Qian, B., Hu, B., & Wang, S. (2023). The Potential of hue angle calculated based on multispectral reflectance for leaf chlorophyll content estimation. *IEEE Transactions on Geoscience and Remote Sensing*. https://doi.org/10.1109/TGRS.2023.3322130

Katahata, S.-I., Naramoto, M., Kakubari, Y., & Mukai, Y. (2007). Seasonal changes in photosynthesis and nitrogen allocation in leaves of different ages in evergreen understory shrub Daphniphyllum humile. *Trees, 21*, 619.

Ke, Y., & Quackenbush, L. J. (2011). A review of methods for automatic individual tree-crown detection and delineation from passive remote sensing. *International Journal of Remote Sensing, 32*, 4725–4747.

Kokaly, R. F., Asner, G. P., Ollinger, S. V., Martin, M. E., & Wessman, C. A. (2009). Characterizing canopy biochemistry from imaging spectroscopy and its application to ecosystem studies. *Remote Sensing of Environment, 113*, S78–S91.

Larsen, M., Eriksson, M., Descombes, X., Perrin, G., & Brandtberg, T. (2011). Comparison of six individual tree crown detection algorithms evaluated under varying forest conditions. *International Journal of Remote Sensing, 32*, 5827–5852.

Li, W., Sun, Z., Lu, S., & Omasa, K. (2019). Estimation of the leaf chlorophyll content using multiangular spectral reflectance factor. *Plant, Cell & Environment, 42*, 3152–3165.

Li, X., Liu, X., Liu, M., Wang, C., & Xia, X. (2015). A hyperspectral index sensitive to subtle changes in the canopy chlorophyll content under arsenic stress. *International Journal of Applied Earth Observation and Geoinformation, 36*, 41–53.

Liaw, A., & Wiener, M. (2002). Classification and regression by randomForest. *R News, 23*, 18.

Lichtenthaler, H. K., & Wellburn, A. R. (1983). Determinations of total carotenoids and chlorophylls a and b of leaf extracts in different solvents. *Analysis, 11*, 591–592.

Louhaichi, M., Borman, M. M., & Johnson, D. E. (2001). Spatially located platform and aerial photography for documentation of grazing impacts on wheat. *Geocarto International, 16*, 65–70.

Ma, L., Zheng, G., Wang, X., Li, S., Lin, Y., & Ju, W. (2018). Retrieving forest canopy clumping index using terrestrial laser scanning data. *Remote Sensing of Environment, 210*, 452–472.

Menze, B. H., Kelm, M. B., Masuch, R., Himmelreich, U., Bachert, P., Petrich, W., & Hamprecht, F. A. (2009). A comparison of random forest and its Gini importance with standard chemometric methods for the feature selection and classification of spectral data. *BMC Bioinformatics, 10*, 1–16.

Meyer, D., Dimitriadou, E., Hornik, K., Weingessel, A., Leisch, F., Chang, C.C., cph], & Lin, C.C. (2015). e1071: Misc Functions of the Department of Statistics, Probability Theory Group (Formerly: E1071), TU Wien

Modica, G., Messina, G., De Luca, G., Fiozzo, V., & Praticò, S. (2020). Monitoring the vegetation vigor in heterogeneous citrus and olive orchards. A multiscale object-based approach to extract trees' crowns from UAV multispectral imagery. *Computers and Electronics in Agriculture, 175*, 105500.

Navarro, A., Young, M., Allan, B., Carnell, P., & Ierodiaconou, D. (2020). The application of Unmanned Aerial Vehicles (UAVs) to estimate above-ground biomass of mangrove ecosystems. *Remote Sensing of Environment, 242*, 111747.

Osco, L. P., Ramos, A. P. M., Pereira, D. R., Moriya, R. A. S., & Creste, J. E. (2019). Predicting canopy nitrogen content in citrus-trees using random forest algorithm associated to spectral vegetation indices from UAV-imagery. *Remote Sensing, 11*, 2925.

Pearson, R. L., & Miller, L. D. (1972). Remote mapping of standing crop biomass for estimation of the productivity of the shortgrass prairie. *Remote Sensing of Environment, 8*, 1355.

Rouse, J., Haas, R., Schell, J., Deering, D., & Harlan, J. (1974). *Monitoring the vernal advancements and retrogradation*. Texas A & M University.

Roussel, J.-R., Auty, D., Coops, N. C., Tompalski, P., Goodbody, T. R., Meador, A. S., Bourdon, J.-F., De Boissieu, F., & Achim, A. (2020). lidR: An R package for analysis of Airborne Laser Scanning (ALS) data. *Remote Sensing of Environment, 251*, 112061.

Santos, A. A. D., Marcato Junior, J., Araújo, M. S., Di Martini, D. R., Tetila, E. C., Siqueira, H. L., Aoki, C., Eltner, A., Matsubara, E. T., Pistori, H., Feitosa, R. Q., Liesenberg, V., & Gonçalves, W. N. (2019). Assessment of CNN-based methods for individual tree detection on images captured by RGB cameras attached to UAVs. *Sensors, 19*, 3595.

Shao, G., Han, W., Zhang, H., Wang, Y., Zhang, L., Niu, Y., Zhang, Y., & Cao, P. (2022). Estimation of transpiration coefficient and aboveground biomass in maize using time-series UAV multispectral imagery. *The Crop Journal, 10*, 1376–1385.

Shao, G., Han, W., Zhang, H., Zhang, L., Wang, Y., & Zhang, Y. (2023). Prediction of maize crop coefficient from UAV multisensor remote sensing using machine learning methods. *Agricultural Water Management, 276*, 108064.

Sims, D. A., & Gamon, J. A. (2002). Relationships between leaf pigment content and spectral reflectance across a wide range of species, leaf structures and developmental stages. *Remote Sensing of Environment, 81*, 337–354.

Sumida, A., Watanabe, T., & Miyaura, T. (2019). interannual variability of leaf area index of an evergreen conifer stand was affected by carry-over effects from recent climate conditions open. *Scientific Reports*. https://doi.org/10.1038/s41598-018-31672-3

Sun, Q., Jiao, Q., Qian, X., Liu, L., & Dai, H. (2021). Improving the retrieval of crop canopy chlorophyll content using vegetation index combinations. *Remote Sensing, 13*, 470.

Team, R.C. (2023). *A language and environment for statistical computing*. R Foundation for Statistical Computing.

Tuia, D., Verrelst, J., Alonso, L., Perez-Cruz, F., & Camps-Valls, G. (2011). Multioutput support vector regression for remote sensing biophysical parameter estimation. *IEEE Geoscience & Remote Sensing Letters, 8*, 804–808.

Ustin, S. L., Gitelson, A. A., Jacquemoud, S., Schaepman, M., Asner, G. P., Gamon, J. A., & Zarco-Tejada, P. (2008). Retrieval of foliar information about plant pigment systems from high resolution spectroscopy. *Remote Sensing of Environment, 113*, S67.

Vélez, S., Martínez-Peña, R., & Castrillo, D. (2023). Beyond vegetation: A review unveiling additional insights into agriculture and forestry through the application of vegetation indices. *J, 6*, 421–436.

Veronika, K., Lucie, K., Jan, J., Zuzana, L., & Filip, O. (2021). Canopy top, height and photosynthetic pigment estimation using parrot sequoia multispectral imagery and the unmanned aerial vehicle (UAV). *Remote Sensing, 13*, 705.

Verrelst, J., Camps-Valls, G., Munoz-Mari, J., Rivera, J. P., Veroustraete, F., Clevers, J., & Moreno, J. (2015). Optical remote sensing and the retrieval of terrestrial vegetation bio-geophysical properties—A review. *Isprs Journal of Photogrammetry & Remote Sensing, 108*, 273–290.

Verrelst, J., Munoz, J., Alonso, L., Delegido, J., Rivera, J. P., Camps-Valls, G., & Moreno, J. (2012). Machine learning regression algorithms for biophysical parameter retrieval: Opportunities for sentinel-2 and -3. *Remote Sensing of Environment, 118*, 127–139.

Vincini, M., & Frazzi, E. (2011). Comparing narrow and broad-band vegetation indices to estimate leaf chlorophyll content in planophile crop canopies. *Precision Agriculture, 12*, 334–344.

Vincini, M., Frazzi, E., & D'Alessio, P. (2007). Comparison of narrow-band and broad-band vegetation indices for canopy chlorophyll density estimation in sugar beet. *Precision Agriculture, 7*, 189–196.

Vincini, M., Frazzi, E., & D'Alessio, P. (2008). A broad-band leaf chlorophyll vegetation index at the canopy scale. *Precision Agriculture, 9*, 303–319.

Wang, S., Li, Y., Ju, W., Chen, B., Chen, J., Croft, H., Mickler, R. A., & Yang, F. (2020). Estimation of leaf photosynthetic capacity from leaf chlorophyll content and leaf age in a subtropical evergreen coniferous plantation. *Journal of Geophysical Research: Biogeosciences, 125*, e2019JG005020.

Wu, C., Zheng, N., Tang, Q., & Huang, W. (2008). Estimating chlorophyll content from hyperspectral vegetation indices: Modeling and validation. *Agricultural and Forest Meteorology, 148*, 1230–1241.

Xue, J., & Su, B. (2017a). Significant remote sensing vegetation indices: A review of developments and applications. *Journal of Sensors, 2017*, 1353691.

Xue, J., & Su, B. (2017b). Significant remote sensing vegetation indices: A review of developments and applications. *Journal of Sensors*. https://doi.org/10.1155/2017/1353691

Zarco-Tejada, P. J., Berjón, A., López-Lozano, R., Miller, J. R., Martín, P., Cachorro, V., González, M., & Frutos, A. D. (2005). Assessing vineyard condition with hyperspectral indices: Leaf and canopy reflectance simulation in a row-structured discontinuous canopy. *Remote Sensing of Environment, 99*, 271–287.

Zhang, Y., Chen, J. M., Miller, J. R., & Noland, T. L. (2008). Leaf chlorophyll content retrieval from airborne hyperspectral remote sensing imagery. *Remote Sensing of Environment, 112*, 3234–3247.

Zhao, D., Raja Reddy, K., Kakani, V. G., Read, J. J., & Carter, G. A. (2003). Corn (*Zea mays* L.) growth, leaf pigment concentration, photosynthesis and leaf hyperspectral reflectance properties as affected by nitrogen supply. *Plant and Soil, 257*, 205–218.